JOURNAL OF OCCUPATIONAL AND ENVIRONMENTAL HYGIENE
2017, VOL. 14, NO. 7, 523–533
https://doi.org/10.1080/15459624.2017.1302587

Taylor & Francis
Taylor & Francis Group

Fume emissions from a low-cost 3-D printer with various filaments

Evan L. Floyd, Jun Wang, and James L. Regens

Department of Occupational and Environmental Health, College of Public Health, University of Oklahoma Health Sciences Center, Oklahoma City, Oklahoma

ABSTRACT

3-D printing is an additive manufacturing process involving the injection of melted thermoplastic polymers, which are then laid down in layers to achieve a pre-designed shape. The heated deposition process raises concerns of potential aerosol and volatile organic compounds (VOC) emission and exposure. The decreasing cost of desktop 3-D printers has made the use of 3-D printers more acceptable in non-industrial workplaces lacking sufficient ventilation. Meanwhile, little is known about the characteristics of 3-D printing fume emission. The objective of this study was to characterize aerosols and VOC emissions generated from various filaments used with a low-cost 3-D printer in an environmental testing chamber. A pre-designed object was printed in 1.25 hours using eight types of filaments. A scanning mobility particle sizer and an aerodynamic particle sizer were employed to measure the particle size distribution in sub-half-micron fraction ($<$0.5 μm) and super-half-micron fraction (0.5–20 μm), respectively. VOC concentration was monitored real-time by a photoionization detector and sampled with a tri-sorbent thermal desorption tube, and analyzed by thermal desorption gas chromatography mass spectrometry (TD-GC/MS). Results showed high levels of fume particles emission rate (1.0×10^7 to 1.2×10^{10} #/min) in the sub-half-micron range with mode sizes of 41–83 nm. Particle concentrations peaked during the heat-up and solid layer printing periods. Total VOC concentration in the chamber followed a first-order buildup, with predominant VOC species in the chamber were breakdown and reaction products of the filaments, such as styrene from ABS filaments. These findings and exposure scenario estimation suggest that although the VOC concentrations were much lower than occupational exposure limits, particles with size less than micron might be a concern for users of low-cost 3-D printers due to high respirablity, especially if used in settings without proper guidance and engineering control.

KEYWORDS
3-D printer; aerosols; volatile organic compounds

Introduction

3-D printing is a type of additive manufacturing and solid freeform fabrication technology. In contrast to the traditional subtractive process of manufacturing by removing material, 3-D printing employs a mechanism in which melted plastic filaments are injected from a nozzle/orifice and are deposited in sequential layers to achieve a pre-designed shape.[1] The emergence of 3-D printing has created an alternative method of precisely manufacturing a solid substance for rapid prototyping and small-scale production.[2] Compared with injection molding and other additive manufacturing processes, 3-D printing enables small-scale and low-cost productions of customized goods and facsimiles. Additional applications of 3-D printing are gaining popularity in the chemical,[3] energy,[4] environmental,[5] medical,[6,7] aerospace,[8] and occupational health[9] fields. Although the 3-D printing community has begun adopting a wider range of printing materials, including metals and ceramics, thermoplastic polymers are still the most utilized filaments, due to their relatively low cost and wider printer compatibility.

Recently, the cost of 3-D printers has significantly dropped due to open-source designs and massive production. While earlier models of 3-D printers could cost as much as $10,000,[10] most small-scale low-cost desktop 3-D printers were priced well under $500 in 2016. Often, low-cost 3-D printers are built on an open frame without any forced ventilation or fume capture devices, in

CONTACT Jun Wang jun-wang@ouhsc.edu Department of Occupational and Environmental Health, College of Public Health, University of Oklahoma Health Sciences Center, P.O. Box 26901, Oklahoma City, OK 73126-0901.
Color versions of one or more of the figures in the article can be found online at www.tandfonline.com/uoeh.
Supplemental data for this article can be accessed at tandfonline.com/uoeh. AIHA and ACGIH members may also access supplementary material at http://oeh.tandfonline.com/.

contrast to commercial 3-D printers, which usually come with enclosures and/or fume traps. This affordable 3-D printing technology has spawned increased applications in small businesses and home projects, where users have limited access to personal respiratory protection and inadequate ventilation for any indoor airborne toxicant.

Filaments used in low-cost 3-D printers and projects are commonly based on either acrylonitrile butadiene styrene (ABS) or polylactic acid (PLA) with several derivations of these, such as polycarbonate ABS (PCABS) for additional mechanical strength, and metal particles like bronze-infilled PLA (Bronze-PLA) that create textures similar to brass. Traditional fabrication polymers, such as nylon (polyamides, PA) and polyethylene terephthalate (PET), are also used as low-cost 3-D printer filaments. Other filaments used as sacrificial structural support are high impact polystyrene (HIPS) and polyvinyl alcohol (PVA). These supporting materials are needed to stabilize object features that abruptly protrude without layers underneath, but are dissolved in a solvent after printing is complete.

While 3-D printing technology has rapidly dropped in cost and performance has improved, research into the health risks from exposure to 3-D printing fume has not progressed to the same extent. Gaseous and aerosol emissions and exposures raise significant health concerns. Volatile organic compounds (VOC) contain various respiratory sensitizers, irritants, mutagens, and carcinogens, but the greater risk from 3-D printing fume may be due to the formation of ultrafine particles (<100 nm),[11] Several studies[12–16] examined the ultrafine particle emissions from earlier models of 3-D printer and found nanoparticles (<100 nm) with an estimated emission factor of 10^8 to 10^{11} #/min or #/gram filament consumption. However, there are still gaps on the aerosol emissions from filaments other than ABS and PLA. More studies are needed to exam other filaments and the other emissions that may pose health risks from 3-D printing. Based on studies conducted in plastic resin manufacturing, 3-D printing fume is hypothesized to consist of polymer breakdown products.[17,18] Some of these breakdown products could lead to health risks. For example, styrene is a VOC that can be metabolized to styrene oxide, which is mutagenic and possibly carcinogenic.[19] Styrene has a permissible exposure limit (PEL) of 100 ppm[20] and a recommended exposure limit (REL) of 50 ppm,[21] and no observable adverse effects level (NOAEL) of 8 ppm.[22] In addition, no study has examined the morphology and combined nano- and micron-sized concentration of the fume particles.

The objective of this study was to characterize the generation of airborne toxicant, specifically aerosols and VOCs, from a low-cost 3-D printer with several previously uncharacterized filaments. An environmental chamber was used to collect the fume emitted from a popular low-cost 3-D printer. Aerosols were characterized by count concentration, morphology, and size distribution from 16.8 nm to 20 μm range. VOCs were characterized as total VOC concentration and speciation using real-time detection and sorbent sampling, respectively. Emission rates and factors based on printed time and object weights were calculated, respectively. The potential occupational risk was conservatively estimated based on a common exposure scenario.

Materials and methods

Testing chamber and 3-D printer

A 3-D printer (Aworldnet A600, Guangzhou, China) based on the widely used Prusa i3 design was employed in this study. The printer was built from a customized kit costing approximately $200. The 3-D printer was equipped with a nozzle head and baseplate with heating capabilities up to 275°C and 110°C, respectively. Emission sampling and measurement were performed in an enclosed transparent glass box chamber with an exterior dimension of 25.4 cm × 30.5 cm × 30.5 cm and an interior volume of 24.8 L. The relatively small size of the chamber permitted an air exchange rate of 16.2 air changes per hour (ACH) with the exhauster and allowed for well-mixed conditions. The nozzle head of the 3-D printer was placed in the center of the box chamber (Figure 1). The feed air inlet of the chamber was connected to the laboratory air supply with in-line water trap, high-efficiency particulate air (HEPA) filter (Whatman HEPA-CAP75, Kent, UK), and activated carbon sorbent trap. The lab air supplied positive pressure to the chamber and was regulated to match the flow rates of the instrumentations. This ensured the test air was free of moisture, particulates, and organic vapors. Therefore, no background deduction is needed when calculating emission rates and factors. The chamber was purged for at least one hour between experiments.

Filaments and printing objects

Eight filament types with diameters of 1.75 mm were used, namely ABS, PLA, PVA, HIPS, PCABS, nylon, bronze-PLA, and PET. The filaments were all directly purchased from commercial 3-D printing stores. Although the filaments have slightly different recommended printing temperatures, the nozzle and baseplate were fixed at 210°C and 70°C, respectively, to reduce the number of experimental variables. The printing temperature was determined by trial runs to make sure all filaments could be extruded at constant rates and printed at acceptable qualities. During the experiment, a pre-designed 39.2 mm × 47.3 mm × 7.9 mm University of Oklahoma

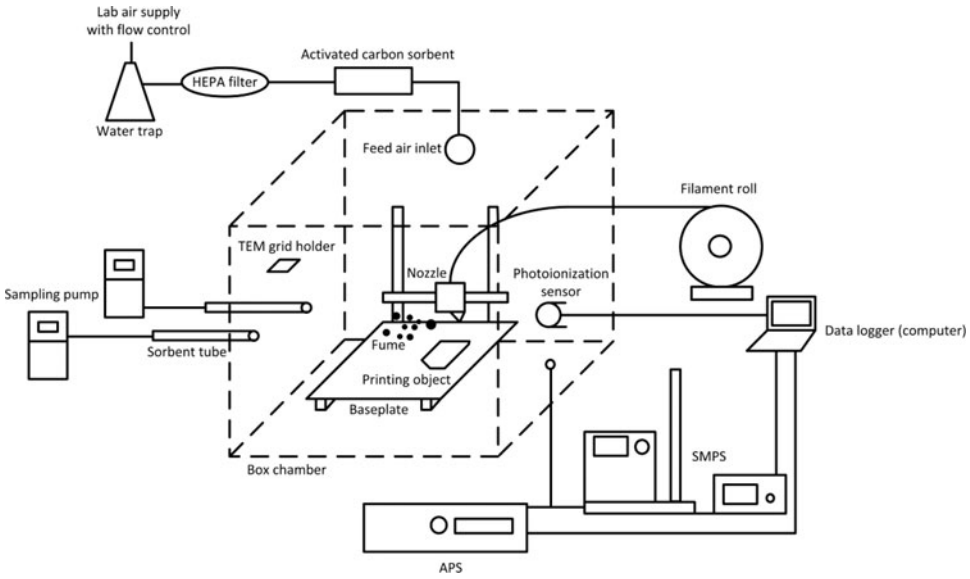

Figure 1. Schematic diagram of the testing chamber.

(OU) logo was printed in 1 hr and 15 min. The logo had a solid shell with a 50% infilled density core. This "porous" structure printing is a common practice with low-cost 3-D printers to conserve filament material. The printed object was weighed using an analytical scale (Mettler Toledo AG-104, Columbus, OH). The gravimetric measurement ensured the mass of printed objects will be similar for each type of filament, and was used for further calculation of emission factors. Details about the filaments' specifications and printing parameters are available in the Supplemental Materials.

Emission measurement and sample analysis

The experimental system is depicted in Figure 1. A scanning mobility particle sizer (SMPS, TSI 3936, Shoreview, MN) and an aerodynamic particle sizer (APS, TSI 3314, Shoreview, MN) were used to measure the fraction of the particles that ranged from 16.8–532.8 nm (referred as "sub-half-micron particle" in this study), and the fraction of the particles ranged from 0.5–20 μm (referred as "super-half-micron particle" in this study), respectively. The measurement interval for both aerosol instruments was synchronized at 1 min. Sampling flow rates of SMPS (1.5 liters per minute, Lpm), APS (5 Lpm), and sorbent tube pumps (0.1 Lpm × 2) resulted in a total ventilation rate of 6.7 Lpm in the chamber. A specialty grid (Pelco 300 mesh, Ted Pella, Redding, CA) was placed onto a holder in the chamber. Transmission electron microscopy (TEM, Hitachi H-7600, Schaumburg, IL) was used to observe the morphology of the fume particles which were passively diffused onto the grid.

A photoionization detector (PID; Baseline VOC-TRAQ, Lyons, CO) was mounted inside the chamber. The PID monitored real-time VOC concentration during printing, with a time resolution of 1 second. Two tri-sorbent sampling tubes (Gerstel, Linthicum Heights, MD) and pumps (SKC Pocket pump 210–1002, Eighty Four, PA) provided a duplicate collection of VOC samples. The flow rate for each pump was set at 0.1 Lpm. 9 L of air were collected with each sorbent tube during each run. The collected samples were then extracted using a thermal desorption system (Gerstel TDS, Linthicum Heights, MD) and were analyzed with a gas chromatograph mass spectrometer (GC/MS, Agilent 6890/5973, Santa Clara, CA). The concentration of speciated VOCs was determined as toluene equivalents following a method combining EPA TO-15[23] and ISO 16000-6 guidelines.[24] Details of the sampling, calibration, and analysis protocol for the above-mentioned instrument can be found in the Supplemental Materials.

An experimental run consisted of: 4 preheating the extruder and baseplate, 75 min of printing, and 11 min of post-printing measurement. The PID monitored VOC concentration changes every second for 5400 sec, while SMPS and APS each recorded 90 measurements throughout the 90-min run. Quadruplicate experiments were conducted for each filament, and results were averaged for all measurements. Printing without actual filaments feeding was conducted as the lab blank. No exceedance of background was found in the blank experiment. Additional details of quality control and statistical analysis are available in the Supplemental Materials.

Calculation of emission rates and factors

Particle count emission rate (#/min) was calculated based on a single loss factor (K_L) that considered surface loss, intra-/inter-coagulation loss, and ventilation loss. The value of K_L was calculated using linear regression from

the natural logarithmic plot of the time-series data during the post-printing period, when emission stopped and loss dominated:

$$K_L = -\frac{\ln(C_{90}/C_{79})}{11}, \quad (1)$$

where C_{90} and C_{79} are the number concentrations at 90 min and 79 min, respectively (#/cm^3). The particle count emission rate ($E_{P\text{-}\Delta t}$) at a given time t (min) was then calculated based on the following equation:

$$E_{P-\Delta t} = V \times \left(\frac{C_{t+1} - C_t}{\Delta t} + K_L \times C_t\right) \quad (2)$$

where C_{t+1} and C_t are the discrete number concentration at time t and t+1, Δt is the sampling interval of 1 min. V is the volume of box chamber (24.8 L). The average emission rate (E_p) during certain periods was calculated based on the summation of the time-varying particle count emission rate ($E_{P\text{-}\Delta t}$):

$$E_p = \frac{\sum E_{P-\Delta t}\Delta t}{t}. \quad (3)$$

In the experiment, two E_P were derived for each filament: $E_{P\text{-high}}$, which represents the high emission rate during the heat up and solid layer printing stage in which particle emission overwhelmingly dominated loss, and $E_{P\text{-total}}$, which represents the averaged emission rate over 77 min of printing time. All count-based emission rates and factors for particles were based on SMPS (sub-half-micron) measurement only, since the number concentration measured by APS (super-half-micron) was later deemed as insignificant.

Total VOC emission rate (µg/min) was calculated based on the first-order buildup eqnarray that assumed that ventilation is the only loss factor for total VOC:

$$E_{VOC} = \frac{C_{79} \times Q}{1 - e^{-\frac{Q}{V}t}}, \quad (4)$$

where E_{VOC} is the emission rate (µg/min), C_{79} is the concentration at 79 min (µg/L), Q is the ventilation rate (6.7 Lpm), V is the volume of box chamber (24.8 L), and t is the total printing time of 77 min.

The generation rate for individual VOC was calculated based on the measured mass in the sorbent tube, using the following equation:

$$G_R = \frac{mQ_t}{tQ_p}, \quad (5)$$

where G is the generation rate (µg/min), m is the measured mass on the sorbents, Q_t is the total ventilation rate (6.7 Lpm), t is the collection time (90 min), and Q_p is the flow rate of the pump (0.1 Lpm).

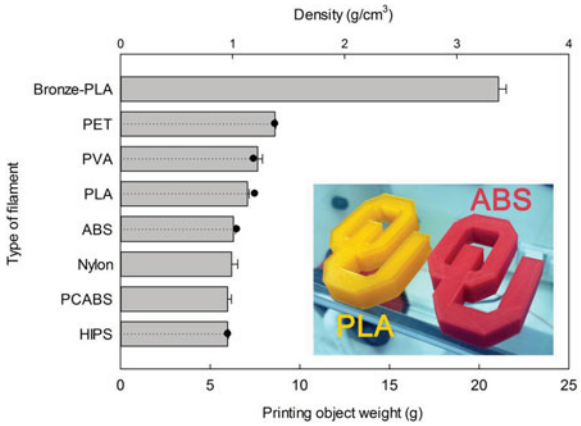

Figure 2. Average weight of printed object for each filament (horizontal bar) with standard deviations (error bar) and known material densities (black dot).

Emission factors based on printed object were calculated using the following eqnarray:

$$EF = \frac{E \times t}{M}, \quad (6)$$

where EF is the emission factor (µg/g of printed object), E is the average emission rate of either particle ($E_{P\text{-}t}$) or VOC (E_{VOC}), t is the total printing time of 77 min, and M is the weight of each printed object.

Results

Printed object weight

Although the dimensions for all printed objects were identical, the objects exhibited differences in mass according to the filament material. Figure 2 shows the averaged weight (M) of the printed objects for each filament. Bronze-PLA had the highest weight of 21.1 ± 0.4 g, while HIPS and PCABS printing were the lowest at 5.9 g ± 0.1 g and 5.9g ± 0.2 g, respectively. Materials with known densities are labeled in Figure 2. The filament vendors did not provide the densities of bronze-PLA, nylon, and PCABS. Bronze-PLA is a metal-plastic polymer composed of PLA and bronze particles. The weight difference between PLA and bronze-PLA should be attributed to the metal in the bronze, i.e. copper (9.0 g/cm^3) and tin (7.3 g/cm^3). Nylon is a group of polyamides with different densities. PCABS is a mixture of polycarbonate and ABS with unknown ratios. Overall, the order of printing object weights is consistent with known material density. It should be noted that the material density is based on 100% purity, while impurities may exist in the consumer-grade 3-D printing filaments.

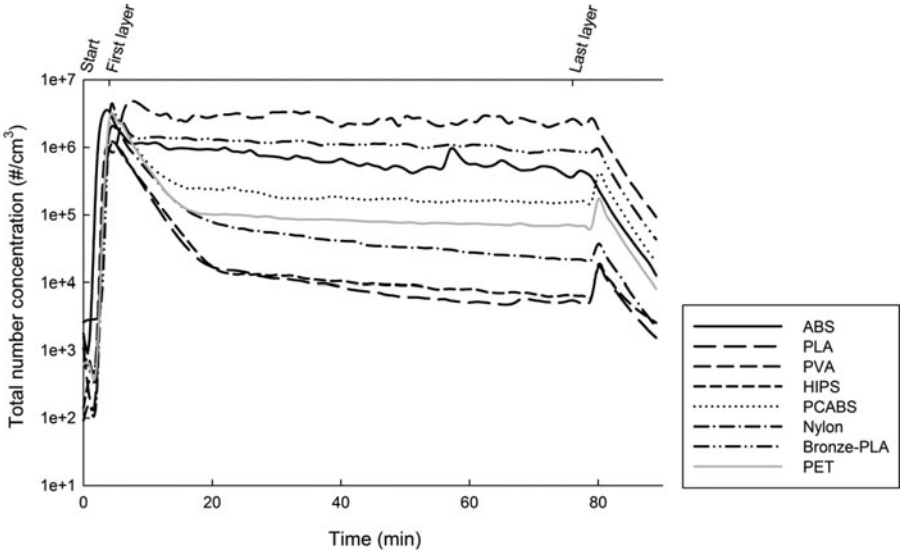

Figure 3. Particle number concentration (#/cm^3) in the sub-half-micron size range (16.8–532.8 nm) as a function of time (min) for each filament.

Particle concentration, size distribution, and morphology

Particle emissions in the sub-half-micron and super-half-micron fractions both increased several orders of magnitude during initial heating and first layer printing stages. Figure 3 shows the averaging total sub-half-micron particle count, illustrated in a time-series fashion. A distinct temporal trend was observed during printing. Particle number reached the maximum during the first four minutes when initial heating occurred (0–2 min) and the solid layer was printed (2–4 min), with an average instantaneous peak concentration between 1.1×10^6 #/cm^3 (PLA & HIPS) and 4.8×10^6 #/cm^3 (PVA) in the SMPS sampling airstream. The sub-half-micron particle concentration for each filament showed slightly different decay trends after the initial burst period. PVA, bronze-PLA, and ABS stayed relatively constant after the initial period, while other filaments slowly dropped over time, when particle loss overwhelmed particle formation. This difference in decay could be due to different particle emission rates for each filament. The particle counts again increased during the last two minutes, when solid printing occurred again. This indicated a high particle emission rate while printing the first and last layers (solid hard-shell), compared with printing the middle layers (50% infilled density core). Hence, the calculation of $E_{P\text{-high}}$ used aggregated data from $t_{2\sim4}$ and t_{75-79} when particle generation dominated particle loss, while calculation of $E_{P\text{-total}}$ used aggregated data of $t_{0\text{-}79}$.

These particle numbers were converted to $E_{P\text{-high}}$ between 0.8×10^{11} #/min (PLA & HIPS) and 4.3×10^{11} #/min (PVA). The $E_{P\text{-total}}$ were one to three orders of magnitude smaller, between 1.0×10^7 #/min (PLA) and 1.2×10^{10} #/min (PVA). $E_{P\text{-H}}$ findings in this study were similar to those of Stephens et al.,[12] who estimated emission rates of 2.0×10^{10} #/min (PLA) and 1.9×10^{11} #/min (ABS). The emission factors based on printed object weights ranged from 1.1×10^8 #/g (PLA) to 1.2×10^{11} #/g (PVA). HIPS, despite having an emission level similar to PLA, had a higher emission factor, due to lower density and therefore lower printed object weight.

Table 1 shows the geometric mean diameter (GMD) based on the number and the geometric standard deviation (σ) for particles emitted at the peak concentration. The PVA sample had the largest GMD of 83.0 nm, while the GMD of other seven filaments ranged from 41.4–55.9 nm. The geometric standard deviations are between 1.5 and 1.8, indicating a single modal distribution in the ultrafine particle range. The particles all fell into the ultrafine range (<100 nm) and potentially have higher toxicity due to high surface area comparing to their larger counterparts. The averaging evolution of sub-half-micron particle size distribution is illustrated in Figure 4. After the peak concentration had occurred during the initial printing, the geometric mean sizes of particles for all filament types began to increase to 100–200 nm due to inter-coagulation and agglomeration, while the total number declined until printing of the solid layer at the end.

The super-half-micron particle measurement showed a burst trend similar to that observed in the sub-half-micron range at the beginning of printing. The particle number began to decline after the ventilation loss began to dominate. The reduction in super-half-micron particle number was identical across the filaments ($p > 0.1$). An aggregated measurement of APS is shown in Figure 5. The APS reading also indicated that larger unmeasurable

Table 1. Sub-half-micron particle and VOC emission characteristics for different filaments.

Filament type	Sub-half-micron particle number concentration (#/cm^3) ±(standard deviation) at peak	GMD (σ) during peaked sub-half-micron particle number concentration	$E_{P\text{-high}}$ (#/min)	$E_{P\text{-total}}$ (#/min)[a]	Particle emission factor (#/g of printed object)	VOC emission rates (μg/min)±(standard deviation)	VOC emission factor (μg/g of printed object)
ABS	$(3.5 \pm 0.4) \times 10^6$	47.4 nm (1.6)	3.2×10^{11}	2.7×10^8	4.2×10^7	63.9 ± 0.5	782.1
PLA	$(1.1 \pm 0.1) \times 10^6$	44.7 nm (1.5)	0.8×10^{11}	0.1×10^8	0.2×10^7	50.1 ± 0.3	545.0
PVA	$(4.8 \pm 0.2) \times 10^6$	83.0 nm (1.8)	4.3×10^{11}	1.2×10^{10}	1.6×10^9	57.9 ± 0.3	583.3
HIPS	$(1.1 \pm 0.2) \times 10^6$	55.9 nm (1.5)	0.8×10^{11}	0.5×10^8	0.9×10^7	46.9 ± 0.5	604.1
PCABS	$(2.6 \pm 0.1) \times 10^6$	41.7 nm (1.6)	1.9×10^{11}	6.0×10^8	1.0×10^8	65.9 ± 0.3	850.0
Nylon	$(2.0 \pm 0.1) \times 10^6$	56.1 nm (1.6)	1.4×10^{11}	1.2×10^8	1.9×10^7	53.5 ± 0.7	664.3
Bronze-PLA	$(3.0 \pm 0.1) \times 10^6$	42.2 nm (1.6)	2.2×10^{11}	3.9×10^9	1.9×10^8	69.6 ± 0.5	254.3
PET	$(2.7 \pm 0.3) \times 10^6$	41.4 nm (1.6)	2.0×10^{11}	2.6×10^8	3.0×10^7	55.0 ± 0.5	491.8

[a] $E_{P\text{-high}}$ used aggregated data from $t_{2\sim4}$ and $t_{75\text{-}79}$ when particle generation was high, while calculation of $E_{P\text{-total}}$ used aggregated data of $t_{0\text{-}79}$. Both $E_{p\text{-high}}$ and $E_{p\text{-total}}$ were based on SMPS measurement only (sub-half-micron range).

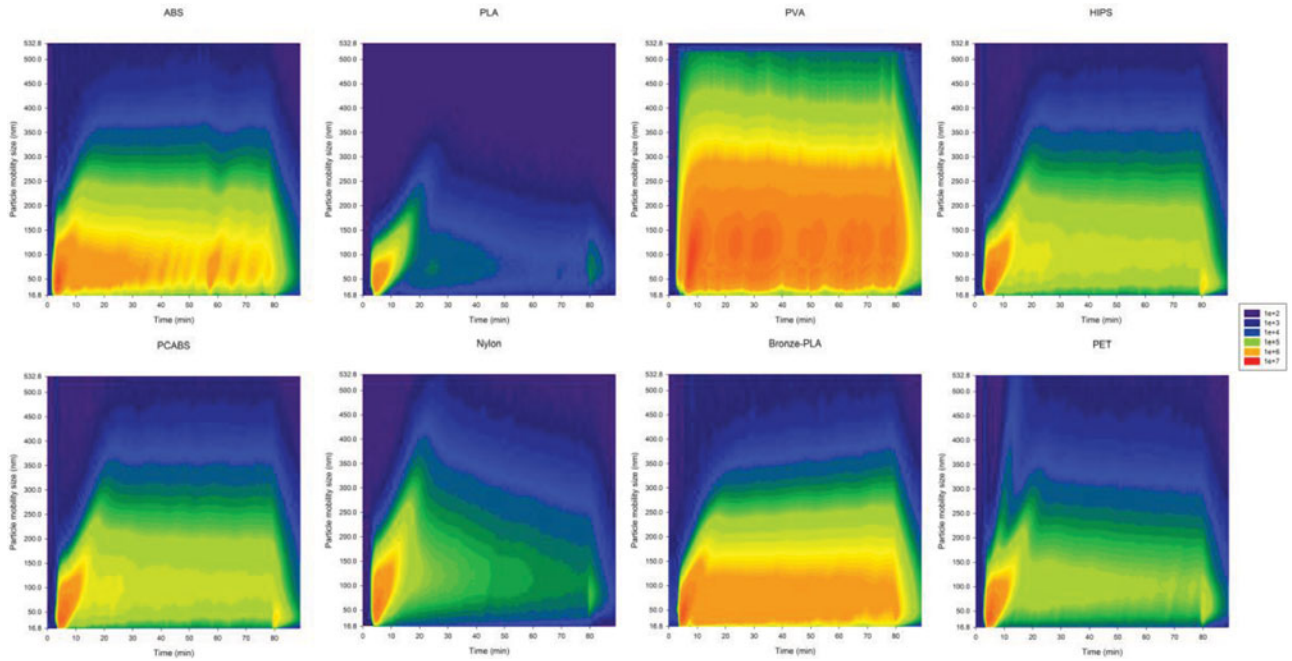

Figure 4. Evolution of particle (mobility) size distribution based on number concentration in the sub-half-micron size range (16.8–532.8 nm) as a function of time (min) for each filament.

quantity of particles saturated the channel of less than 0.5 µm, which is consistent with the sub-half-micron particle measurement. This finding indicated a single modal particle size distribution over the full measurement range of 16.8 nm to 20 µm, with the mode primarily in the ultrafine range.

TEM imaging was similar for particles generated from different filaments. Figure 6 displays typical fume particles on different scales. Figure 6a depicts the primary particles with a size under 100 nm. Figure 6b shows a typical large aggregate formed from primary particles. Figure 6c presents a variety of rod-shaped 3-D printing filaments fragments with aggregated particles attached to the rod.

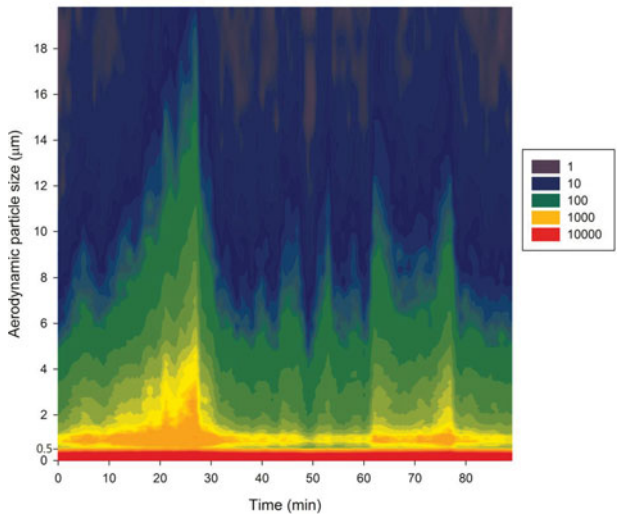

Figure 5. Average evolution of particle (aerodynamic) size distribution based on number concentration in the super-half-micron size range (0.5–20 µm) as a function of time (min).

VOC concentration and speciated VOC profile

The averaging total VOC concentration in the box chamber as a function of time followed a first-order buildup during the first 79 min of printing (Figure 7). VOC concentration then began to decay after the print job stopped. Bronze-PLA printing created the highest VOC concentration in the chamber of 1.1×10^{-2} µg/cm^3. The two ABS-based printing filaments (PCABS and ABS) gave the next highest VOC concentrations of 1.0×10^{-2} µg/cm^3 and 0.9×10^{-2} µg/cm^3 at the end of printing, respectively. HIPS, which is also a styrene-based polymer, produced the lowest VOC concentration of 0.7×10^{-2} µg/cm^3.

The emission rate for each filament is listed in Table 1. Average VOC emission rates ranged from 46.9 µg/min (HIPS) to 69.6 µg/min (Bronze-PLA). Although there are no other comparable published data from studies of 3-D printers, this finding is in the higher end of VOC emission range from other small electronic office devices.[25] The emission factors normalized to printed object weights were between 254.3 µg/g (Bronze-PLA) to 850.0 µg/g (PCABS). The weight-based emission factor indicated an off-gas rate of 0.03– 0.09% while printing. The detectable VOC species in each sample were identified and listed in the Supplemental Materials. The top three VOC by weight percentage were used as marker compounds and the markers' average generation rates for each filament are summarized in Figure 8. Styrene

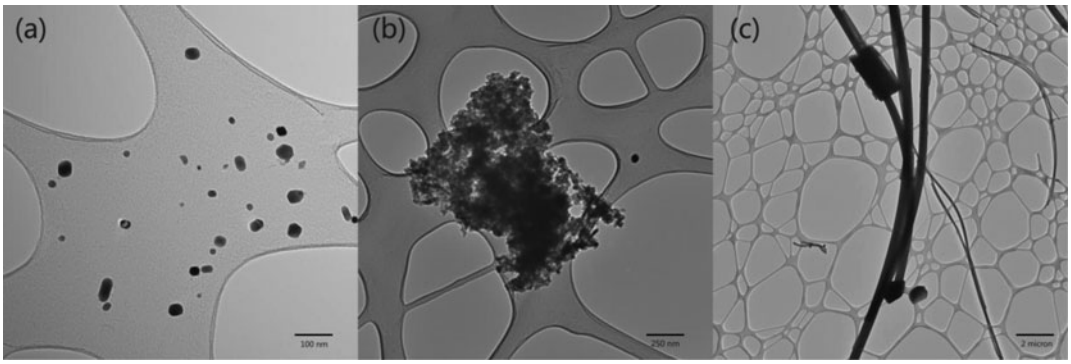

Figure 6. TEM images of fume particles on scales of: (a) 100 nm, (b) 250 nm, and (c) 2 μm.

was found in ABS, HIPS, and PCABS printing samples with generation rates of 4.8 μg/min, 2.6 μg/min, and 21.2 μg/min, respectively. PCABS printing also generated α-methylstyrene with an emission rate of 21.5 μg/min. PLA and bronze-PLA printing both emitted acrylic acid dimer (1,4-dioxane-2,5-dione, 3,6-dimethyl-) at rates of 6.0 μg/min and 11.0 μg/min, respectively. PVA emissions were primarily glycerin (14.2 μg/min), while nylon emissions were primarily caprolactam (26.1 μg/min). PET printing had the lowest emission rate of the top three markers (2.1 μg/min). It should be noted that the individual VOC emission results were semi-quantitative, since the individual VOC mass was quantified using a toluene equivalent method. A styrene recovery test showed a near 100% efficiency for styrene, which has a similar molecular structure to toluene and was the most toxic substance identified in this study.

Discussion

Aerosol emission

A relatively large and small burst of particle number concentration occurred during the initial printing and the finishing, respectively. This may be due to the pre-heating and printing of 100% solid layers for the solid exterior of the objects. The particle concentration declined at different rates during the printing. These declining trends indicated a lower emission rate than ventilation rate when printing the 50% infilled density layer compared with the solid exterior layers. Although most low-cost 3-D printer users will likely choose to print objects that are more "porous" in order to save on materials, the earlier model and commercial 3-D printer typically print high solidity objects for better mechanical properties, which may sustain elevated particle emission rates.

Regarding both concentration and size distribution, the particle profiles were in the same range of that of small electric devices like laser-jet printers.[26] The size distribution of the particles raised concerns of nanoparticle exposure during printing. Although there is no exposure regulation based on particle size or number, a large number of particles emitted at magnitudes of 10^{11} #/min during peak, combined with a modal size of less than 100 nm, favors the particles penetrating to the alveolar

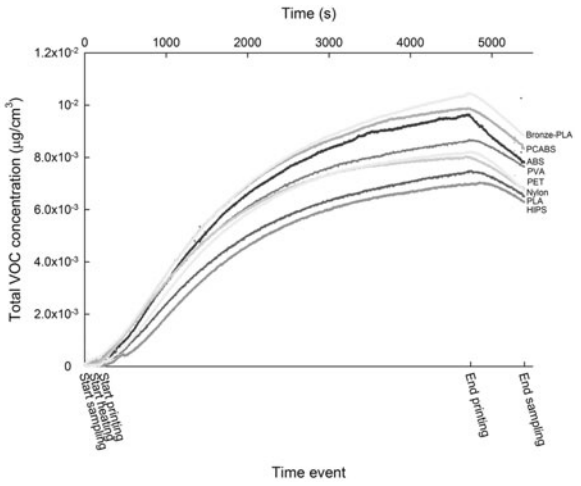

Figure 7. Total VOC concentration (μg/cm^3) in the chamber measured by photoionization sensor.

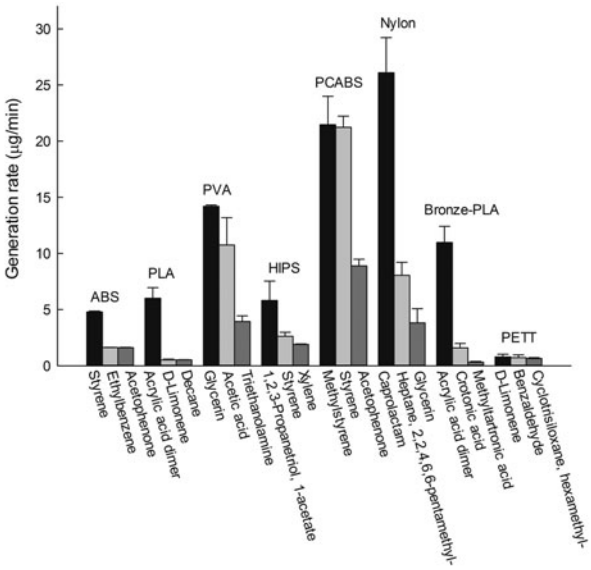

Figure 8. Generation rate (μg/min) with standard deviations (error bar) of top three VOC markers for each filament.

region of the respiratory tract. The differences between the concentrations measured in the present study and those estimated by other studies[12–15] could be attributed to differences in experimental design, such as print rates, printer settings (temperature and printing speed), filament quality, pigments in the filament, and environmental conditions. Most notably, the printing time in previous studies was much shorter (~20 min), and the infilled density is unknown. This shorter print time could lead to a higher ratio of printing solid layers to hollow layers, and could cause particle number burst. In addition, Stephens et al.'s study[12] was based on a worst-case scenario in offices, rather than direct measurements. Thus, particle concentration may have been overestimated.

The particle morphology images again confirmed the existence of primary sub-half-micron particles and secondary super-half-micron particles. The presence of micron-sized rod-shaped filament fragments is previously unreported, and could play an important role in scavenging smaller particles such as those in the sub-half-micron range. In addition, the rod-shaped fragments can pose more pulmonary risks due to the ability to be trapped in the small airways.

VOC generation during 3-D printing

The first-order buildup curve shown in Figure 5 indicates a relatively constant VOC generation rate for each filament throughout the printing process. The total VOC emission rate of the highest filament (Bronze-PLA) is 50% higher than that of the lowest filament (HIPS). The combination of bronze particles and pure PLA material might play an important role in releasing more vapors at high temperature, from both physical material bonding and chemical catalysis by copper and tin. PCABS and ABS printing can usually provide better mechanical properties than other filaments, especially the most widely used PLA, but with approximately 30% higher emission rates (63.9 μg/min for ABS and 65.9 μg/min for PCABS versus 50.1 μg/min for PLA). HIPS had the lowest VOC emission rate. However, HIPS is unlikely to be used alone as a 3-D printing filament since it is recognized as a supporting material for other filaments.

The speciated VOC information is more critical than the total VOC emission rate, since the toxicity of VOCs varies widely from compound to compound. As expected, styrene and its derivatives were the predominant VOCs for the styrene-based filaments (ABS, PCABS, and HIPS). PCABS emitted both α-methylstyrene and styrene. Styrene is well known for its toxicity, and multiple exposure limits have been established against it. α-methylstyrene is commonly found in the production of high strength and impact-resistant ABS resin.[27] An animal study conducted by the National Toxicology Program (NTP) showed increased incidences of renal tubule adenomas and carcinomas in rats after exposure to α-methylstyrene.[28] Considering that PCABS also had the second highest total VOC emission rate (65.9 μg/min) among the 8 filaments tested, printing with PCABS may present the highest risk of adverse health effects. Ethylbenzene, found in ABS printing, is listed as a possible carcinogen by IARC,[19] with exposure resulting in increased incidences of kidney and testicular tumors in rats. Acetophenone is another suspected breakdown product, likely derived from styrene. Although it is not classified as a carcinogen, one study showed that acetophenone can induce chromosomal damage and mutagenesis.[29]

Acrylic acid dimer was the primary marker for PLA-based filaments indicating thermally induced dehydration of lactic acid into acrylic acid and subsequent dimerization.[30] Other speciated VOC emissions from PLA-based filaments were at trace levels and non-toxic. For example, *d*-limonene is a safe flavoring agent and even has chemopreventive potential against some cancers.[31] The VOC speciation verified the safety advantages of PLA-based filaments over ABS-based filaments, as many PLA filaments are marketed as "biodegradable" and "safer" filaments.

Other significant markers included glycerin in PVA and nylon printing. Glycerin is a sugar-alcohol compound that is widely used in pharmaceutical synthesis. Caprolactam is a cyclic amide and precursor of nylon 6, with ambiguous toxicity. Benzaldehyde, which is a hazardous substance listed by the EPA[32] was emitted during PET printing at an extremely low rate (0.7 μg/min). In summary, most emitted VOCs were either the direct breakdown or converted products of original filament material. Printing with ABS-derived filaments had much higher toxic emissions than other filaments.

Exposure scenario estimation

Although this study was conducted in an environmental testing chamber and should not be directly compared to the established exposure limits, it is still useful to estimate the risks based on a common exposure scenario, i.e., regular ventilation dilution with no local exhaust ventilation and a single 3-D printer. Styrene was selected as a primary representative compound, since its limits and toxicological evidence are well established. The styrene emission rate for ABS-based filaments can be as high as 21.2 μg/min during PCABS printing. In this scenario, continuously printing with PCABS will result in an 8-hr time-weighted average (TWA) environmental concentration of 2.0×10^{-4} μg/cm^3 in an average room size of 50 m^3, without any ventilation dilution. This environmental concentration was insignificant compared with either the short-term exposure limit PEL (100 ppm, 0.425 μg/cm^3)

or the 8-hr TWA PEL (50 ppm, 0.215 μg/cm^3),[20] although the values should not be compared directly. We also estimated risk for ethylbenzene, which has a similar PEL (100 ppm, 0.435 μg/cm^3)[33] and even lower emission rates from ABS printing (1.6 μg/min).

The exposure estimation and comparison was not practicable for ultrafine aerosols, since there is no exposure standard based on particle number concentration.[34] However, using a number-to-mass conversion with assumed density from the filament material showed an estimated 8-hr TWA exposure to ultrafine aerosols of up to 41 μg/m^3 (PVA printing continuously in a 50-m^3 room with limited ventilation). This is just over the EPA $PM_{2.5}$ 24-hr limit of 35 μg/m^3 limit and may be more appropriate when considering the potential for non-occupational exposures to 3-D printer fumes. While the 3-D printer user should be cautious of high concentrations of nanoparticles emitted during printing, proper guidance and engineering controls to reduce the exposure to particles should be made available to users. Studies of the potential health risk of 3-D printing fume should emphasize ultrafine aerosol and its chemical composition, especially its bioavailability. It should be noted the rod-shaped particles will contribute to overall toxicity due to their similarity to fibers. It is difficult to apply the traditional industrial hygiene hierarchy based on regulation and control in this scenario, due to the lack of exposure limits. Control banding is an alternative model with which to categorize the risks and apply corresponding controls for nanoparticle exposure scenarios like low-cost 3-D printing.[35]

Conclusions

This study successfully characterized the profile of 3-D printing fume emissions, i.e., particle number concentration (#/cm^3), emission rate (#/min), and emission factor (#/g). The single modal particle distribution with the mode size in the ultrafine range indicated a potential exposure for users of low-cost 3-D printers to high concentrations of nanoparticles. ABS-based filament (ABS and PCABS), bronze-PLA, and PVA produced the highest emission of particles. Total VOC emission rate and factors, as well as the top VOC compounds based on weight percentage were identified.

Future research should incorporate more speciated studies on ultrafine aerosols from 3-D printing, since ultrafine aerosols pose greater health risks than larger particles. Other gaseous toxins in the aerosol may lead to serious adverse health effects. Field studies should be conducted to evaluate the actual user exposure as well as the effectiveness of potential engineering controls. *In vitro* and *in vivo* toxicological studies will be helpful, as 3-D printing fume is a mixture of different chemicals and it is difficult to determine the toxic effects solely based on the composition of fume. Post-printing procedures, including wax infiltration and air blow cleaning, may also generate secondary emissions and exposures.

Acknowledgment

The authors would like to thank the Oklahoma Medical Research Foundation (OMRF) for providing instrumental access to the TEM.

Funding

This study was partially funded by the Presbyterian Health Foundation (PHF).

References

[1] **Sachs, E., M. Cima, and J. Cornie:** Three-dimensional printing: Rapid tooling and prototypes directly from a CAD model. *CIRP Ann. Manuf. Technol. 39*(1):201–204 (1990).

[2] **Baraniuk, C.:** Beyond 3D printing: The all-in-one factory. *New Sci. 219*(2930):20 (2013).

[3] **Kitson, P.J., M.D. Symes, V. Dragone, and L. Cronin:** Combining 3D printing and liquid handling to produce user-friendly reactionware for chemical synthesis and purification. *Chem. Sci. 4*(8):3099–3103 (2013).

[4] **Arenas, L.F., F.C. Walsh, and C.P. de León:** 3D-printing of redox flow batteries for energy storage: a rapid prototype laboratory cell. *ECS J. Soild State Sci. Technol. 4*(4):P3080–P3085 (2015).

[5] **Kreiger, M., and J.M. Pearce:** Environmental impacts of distributed manufacturing from 3-D printing of polymer components and products. *MRS Online Proc. Lib. 1492*:85–90 (2013).

[6] **Warnke, P.H., H. Seitz, F. Warnke, et al.:** Ceramic scaffolds produced by computer-assisted 3D printing and sintering: Characterization and biocompatibility investigations. *J. Biomed. Mat. Res. Part B Appl. Biomater. 93B*(1):212–217 (2010).

[7] **Zhao, L., V.K. Lee, S.-S. Yoo, G. Dai, and X. Intes:** The integration of 3-D cell printing and mesoscopic fluorescence molecular tomography of vascular constructs within thick hydrogel scaffolds. *Biomaterials 33*(21):5325–5332 (2012).

[8] **NASA:** "3D Printer Headed to Space Station." Available at https://www.nasa.gov/content/3d-printer-headed-to-space-station.

[9] **Joe, P.S., P.C. Shum, D.W. Brown, and C.T. Lungu:** A novel method for designing and fabricating low-cost facepiece prototypes. *J. Occup. Environ. Hyg. 11*(10):665–671 (2014).

[10] **Berman, B.:** 3-D printing: The new industrial revolution. *Bus. Horiz. 55*(2):155–162 (2012).

[11] **Biswas, P., and C.-Y. Wu:** Nanoparticles and the environment. *J. Air Waste Manage. Assoc. 55*(6):708–746 (2005).

[12] **Stephens, B., P. Azimi, Z. El Orch, and T. Ramos:** Ultrafine particle emissions from desktop 3D printers. *Atmos. Environ. 79*(0):334–339 (2013).
[13] **Afshar-Mohajer, N., C.-Y. Wu, T. Ladun, D.A. Rajon, and Y. Huang:** Characterization of particulate matters and total VOC emissions from a binder jetting 3D printer. *Build. Environ. 93*(Part 2):293–301 (2015).
[14] **Kim, Y., C. Yoon, S. Ham, et al.:** Emissions of nanoparticles and gaseous material from 3D printer operation. *Environ. Sci. Technol. 49*(20):12044–12053 (2015).
[15] **Azimi, P., D. Zhao, C. Pouzet, N.E. Crain, and B. Stephens:** Emissions of ultrafine particles and volatile organic compounds from commercially available desktop three-dimensional printers with multiple filaments. *Environ. Sci. Technol. 50*(3):1260–1268 (2016).
[16] **Steinle, P.:** Characterization of emissions from a desktop 3D printer and indoor air measurements in office settings. *J. Occup. Environ. Hyg. 13*(2):121–132 (2016).
[17] **Contos, D.A., M.W. Holdren, D.L. Smith, R.C. Brooke, V.L. Rhodes, and M.L. Rainey:** Sampling and analysis of volatile organic compounds evolved during thermal processing of acrylonitrile butadiene styrene composite resins. *J. Air Waste Manage. Assoc. 45*(9):686–694 (1995).
[18] **Unwin, J., M.R. Coldwell, C. Keen, and J.J. McAlinden:** Airborne emissions of carcinogens and respiratory sensitizers during thermal processing of plastics. *Ann. Occup. Hyg. 57*(3):399–406 (2013).
[19] **IARC:** "Monographs on the Evaluation of Carcinogenic Risks to Humans." Available at http://monographs.iarc.fr/.
[20] **OSHA:** Styrene. In *Toxic and Hazardous Substances*, Occupational Safety and Health Standards, Washington, DC: US Department of Labor, 2006.
[21] **NIOSH:** *Pocket Guide to Chemical Hazards*. Cincinnati, OH: NIOSH, 1997.
[22] **USEPA:** *Integrated Risk Information System (IRIS) on Styrene*. Washington, DC: USEPA, 1999.
[23] **EPA:** TO-15 Determination of VOCs in air collected in specially prepared canisters and analyzed by gas chromatography mass spectrometry (GCMS). EPA 625/R-96/010b. Washington, DC: USEPA, 2009.
[24] **ISO:** ISO 16000-6:2011: Indoor Air- Part 6: Determination of Volatile Organic Compounds in Indoor and Test Chamber air by Active Sampling on Tenax TA Sorbent, Thermal Desorption and Gas Chromatography using MS or MS-FID. Berlin: Beuth Verlag, 2011.
[25] **Lee, S.C., S. Lam, and H. Kin Fai:** Characterization of VOCs, ozone, and PM10 emissions from office equipment in an environmental chamber. *Build. Environ. 36*(7): 837–842 (2001).
[26] **Schripp, T., M. Wensing, E. Uhde, T. Salthammer, C. He, and L. Morawska:** Evaluation of ultrafine particle emissions from laser printers using emission test chambers. *Environ. Sci. Technol. 42*(12):4338–4343 (2008).
[27] **Zhu, W., and J. Zhang:** Mechanical and thermal properties of (acrylonitrile-styrene-acrylic)/(α-methylstyrene-acrylonitrile) binary blends. *J. Vinyl Add. Tech. 22*(2):156–162 (2016).
[28] **NTP:** "NTP Technical Report on the Toxicology and Carcinogenesis Studies of Alpha-methylstyrene in F334/N Rats and B6C3F1 Mice (Inhalation Studies)." Research Triangle Park, NC: National Institutes of Health, 2007.
[29] **Fix, D., and R. Bockrath:** Targeted mutation at cytosine-containing pyrimidine dimers: studies of Escherichia coli B/r with acetophenone and 313-nm light. *Proc. Natl. Acad. Sci. U.S.A. 80*(14):4446–4449 (1983).
[30] **Lira, C.T., and P.J. McCrackin:** Conversion of lactic acid to acrylic acid in near-critical water. *Ind. Eng. Chem. Res. 32*(11):2608–2613 (1993).
[31] **Sun, J.:** D-limonene: safety and clinical applications. *Altern. Med. Rev. 12*(3):259–264 (2007).
[32] **EPA:** "Integrated Risk Information System (IRIS): Benzaldehyde (CASRN 100-52-7)." Available at http://www.epa.gov/iris/subst/0332.htm.
[33] **OSHA:** Ethylbenzene. In: *Toxic and Hazardous Substances*. Occupational Safety and Health Standards. Washington, DC: US Department of Labor, 2006.
[34] **Schulte, P.A., V. Murashov, R. Zumwalde, E.D. Kuempel, and C.L. Geraci:** Occupational exposure limits for nanomaterials: state of the art. *J. Nanopart. Res. 12*(6):1971–1987 (2010).
[35] **Brouwer, D.H.:** Control banding approaches for nanomaterials. *Ann. Occup. Hyg. 56*(5):506–514 (2012).